N87-26012

APPLICATIONS OF COMPUTATIONAL MODELING IN BALLISTICS

Walter B. Sturek
US Army Ballistic Research Laboratory, LABCOM
Aberdeen Proving Ground, Maryland 21005-5066

ABSTRACT

The development of the technology of ballistics as applied to gun launched Army weapon systems is the main objective of research at the US Army Ballistic Research Laboratory. The primary research programs at the BRL consist of three major ballistics disciplines: exterior, interior and terminal. The work done at the BRL in these areas has traditionally been highly dependent on experimental testing. A considerable emphasis has been placed on the development of computational modeling to augment the experimental testing in the development cycle; however, the impact of the computational modeling to this date has been modest. With the availability of supercomputer computational resources recently installed at the BRL, a new emphasis on the application of computational modeling to ballistics technology is taking place. The intent of this paper is to outline the major application areas which are receiving considerable attention at the BRL at present and to indicate the modeling approaches involved. An attempt has been made to give some information as to the degree of success achieved and indicate the areas of greatest need.

INTRODUCTION

The development of ballistics technology as applied to gun launched Army weapons systems is the main objective of research at the US Army Ballistic Research Laboratory. The primary research programs at the BRL consist of three major ballistics disciplines: exterior, interior and terminal. The work done at the BRL in the areas has traditionally been highly dependent on experimental testing. A considerable emphasis has been placed on the development of computational modeling to augment the experimental testing in the development cycle; however, the impact of the computational modeling to this date has been modest. This has been primarily caused by the lack of adequate computational resources at the BRL which has relied on a CDC 7600 computer since 1975. The CDC 7600 computer was replaced by a Cray XMP/48 computer in December 1986.

With the considerable increase in computational capability provided by this computer, a new emphasis on the application of computational modeling to ballistics technology is taking place. The intent of this paper is to outline the major application areas which are receiving considerable attention at the BRL at present and to indicate the modeling approaches involved. An attempt has been made to give some information as to the degree of success achieved and indicate the areas of greatest need.

Since the three ballistic disciplines represent well defined work areas, each discipline is discussed separately in the paper in the order: exterior, interior and terminal.

Exterior Ballistics

The computational modeling of exterior ballistic flows at BRL has been very active since 1973. More recently, the application of the thin layer, Navier-Stokes computational codes developed by Pulliam and Steger[1] and Schiff and Steger[2] have been applied to a variety of projectile flow fields at transonic and supersonic velocities. Our early efforts focused on the validation of the computational codes by making detailed comparisons with experimental data which were obtained for that express purpose. This code validation phase was carried out over the time period from 1975 to 1983. During this time period, the ability to predict the Magnus characteristics of spinning shell at supersonic velocities was confirmed. The Magnus coefficient is the critical parameter since it is a viscous effect and is 1/10th to 1/100th of the normal force. Figure 1 shows an illustration of the forces acting on an artillery shell. Thus, if the Magnus force can be predicted correctly, all the other static aerodynamic coefficients can also be predicted accurately.

The Aerodynamics of Spinning Shell

The critical aerodynamic behavior for a spinning artillery shell occurs in the transonic velocity regime. This critical behavior occurs between Mach = 0.9 and 1.0 and results in the gyroscopic stability of the shell being at a minimum where the Magnus moment and pitching moment are at a maximum. Figure 2 shows the expected behavior of the pitching moment coefficient as a function Mach number. Since the Magnus pitching moments have maximum values at some subsonic Mach number between 0.9 and 1.0, the determination of these coefficients is of greatest interest in this speed range. Unfortunately, this is the speed range which requires the greatest computational resources.

The geometry of a typical artillery shell, shown in Figure 3, consists of an ogive forebody with a flattened nose, cylindrical midbody and a boattailed afterbody. The flowfield for this type of shell at a transonic Mach number of 0.94 is shown as a spark shadowgraph from the BRL Transonic Range in Figure 4. The flowfield is shown to consist of significant regions of subsonic and supersonic flow, shock-boundary layer interactions, and separated flow at the base of the projectile. The modeling of this flowfield is further complicated by the loss of pitch plane symmetry that occurs due to the effect of surface spin. In order to model this flowfield, three-dimensional, time-marching, Navier-Stokes computational techniques are required.

The flowfield for a projectile in flight at supersonic velocity is shown in Figure 5. The characteristic of this flowfield of particular interest here is that the effect of flowfield disturbances are only felt downstream. Thus the Parabolized Navier-Stokes (PNS) computational

technique can be applied. The computational technique has been very successful at predicting the aerodynamic behavior of spinning shell including the Magnus effect. These results have been extensively reported[3] and will not be discussed further here.

Several papers have been written over the past five years describing our attempts to predict the aerodynamic coefficients at transonic velocities.[4-5] Figure 6 shows the results achieved on a Cray 1 using two million words of memory. The peak value of the pitching moment is about right; however, the trend of the coefficient with Mach number is unsatisfactory. Our latest attempt, which has not yet been published, was recently completed on the X-MP/48 at the NASA Ames Research Center. This computation took a year to complete due to problems of remote access, file storage and CPU availability. In order to carry out the full computation in which the entire projectile with the base region and the effect of surface spin are included, we expect to require at least eight million words of memory. The CPU time on an X-MP/48 using a fully vectorized code is expected to be of the order of 45 hours. This is the time using a single processor. It is obvious that to achieve improved turnaround time, the ability to perform computations on multiple processors is important.

Base Flow Modeling

Base region flowfield computations at zero angle of attack have been performed at BRL for several years. The results of these computational studies have been reported in References 6 and 8. The technique uses the thin-layer, time-marching Navier-Stokes computational code as reported by Nietubicz, Pulliam and Steger.[7] An important feature of the technique is the ability to preserve the sharp corner at the base of the projectile. This is achieved using a zonal gridding approach.

An example of the application of this predictive capability to current projectile development concerns is shown in Figure 7 where two examples of irregular base region configurations are shown. These base configurations are currently being considered as modifications for fielded Army shell. The configurations are known to have measurable effects on the flight performance of the shell. Computational studies are underway to predict the total drag of the shell using the axisymmetric Navier-Stokes computational code. Using the X-MP class of machine, a substantial matrix of results can be developed over the speed range of interest, $.8 < M < 2.5$. An example of recent results achieved is shown in Figure 8 where the total drag for the standard and modified base geometries are plotted versus Mach number. Full 3D simulations are desired in order to provide the complete aerodynamic performance; however, the scope of results needed and the timeframe involved make this achievement unattainable.

The base flow modeling has been also been extended to include mass injection into the base region.[8] This capability is desired to predict the performance of rocket assist and base bleed shell. The current configuration of the XM864 base bleed shell is shown in Figure 10 as an example. Recent results achieved in the modeling of this type of flow is shown in Figure 9 where the mass injected is modeled as a perfect gas. This figure compares the computation to an experiment conducted for the US Army Missile Command at AEDC. The results show comparisons of surface pressures at the base of the model. These results are encouraging; however, the real problem includes effects of multi-phase flow with combustion. The modeling of these effects is of considerable interest and research in this area is in progress.

Finned Projectiles

Kinetic energy penetrator projectiles are of considerable development interest within the Army. These are long L/D, finned projectiles which are launched at high supersonic velocities ($M > 4.5$) and have a very short time-of-flight (3-4 seconds maximum). A simplified drawing of a typical fielded round (M735) is shown in Figure 10. A spark shadowgraph taken in the BRL Transonic Range of this projectile in flight at Mach = 4.5 is shown in Figure 12.

A series of computational studies for this type of projectile have been carried out using the PNS computational technique and are reported in Reference 9 and 10. Figure 13 shows the development of particle traces at the surface of the projectile in the vicinity of the fins. A comparison between the computations and free flight measurements of pitching moment is shown in Figure 14. In an attempt to achieve better comparisons with the experimental measurements, computations have been made with highly dense grids in the vicinity of the fins by coupling solutions from PNS and time-marching techniques. The results achieved indicate some improvement; however, further improvement in the ability to predict the aerodynamics of these shapes await the impact of greater computational resources than has been used to this date. This is especially true since current interest is in projectiles with L/D's greater than 20.

Interior Ballistic Modeling

The interior ballistic cycle involves the combustion of solid propellant in a gun tube which creates the high pressure required to propel the projectile out of the gun tube into free flight. The time of the cycle is of the order of 10-15 milliseconds. The maximum pressures reached are of the order of 50,000 psi and the flame temperature of the burning gases is of the order of 2500 R. The configuration of the propellant consists of rods or sticks which are packaged together to form a loosely packed bundle or multiple bags of material.

The ignition of the propellant is a very important aspect of the burning since the pressure-time behavior of the combustion process can, if too violent, result in the destruction of the breech of the gun. Thus, the interior ballistic problem has the following characteristics: (1) time dependent; (2) multi-phase flow (solid and gaseous); (3) combustion; (4) high temperature; (5) high pressure; (6) real gas effects; (7) chemically reacting gas.

Due to the highly complex nature of the interior ballistics problem, current computational modeling techniques are far from being able to adequately model the full physical processes of interest. Thus, current computational modeling[11-12] makes use of a combination of lumped parameter, two dimensional-two phase flow, quasi-one dimensional flow modeling and modified constitutive laws for chemical energy release, frictional losses, heat loss to the gun tube and erosive burning. A schematic illustration of a bagged charge inside of a gun chamber is shown in Figure 15. This drawing shows the basic configuration of the interior ballistic problem prior to ignition. A schematic illustration of the configuration for a multi-increment charge is shown in Figure 16. The presence of considerable ullage (or empty space) is illustrated and is an important factor in the performance of the propellant. The combination of modeling techniques used to model this multi-increment configuration is shown in Figure 17.

Terminal Ballistic Modeling

The terminal ballistics problem consists of several processes including: response of structures such as vehicles and shelters to blast waves, penetration of armor by long rod projectiles and penetration of armor by high velocity plasma jets.

Armor Penetration

There are a number of penetration and impact codes which have been developed. Eight such codes are surveyed in Reference 13. EPIC-3[14] is actively used at BRL. EPIC-3 is a finite element code in a Lagrangian formulation. Models for material properties and equations of state to account for high energy impact are an important part of the computational technique. An example of an EPIC-3 computation for impact of a steel ball onto an aluminum plate is shown in Figure 18. Excellent agreement with experiment has been obtained for this case.

Another code used extensively at BRL for armor penetration modeling is the EPIC-2 code.[15] An example of the application of this code to predict the penetration of single plate armor by a long rod is shown in Figure 19. In this figure, examples are shown of the time-dependent armor penetration process for two angles of impact, normal and oblique to the surface. The modeling of the armor penetration process is accomplished by a combination of Lagrangian and Eulerian techniques. Modeling of the dynamic response of the target material to the high energy release is an important aspect of this computational technique. The full problem of interest requires the capability to model penetration of multiple armor plates at high angles of obliquity. Fully three-dimensional computations require considerable computer resources in terms of CPU time and storage capacity.

Incident Blast Wave Effects

Blast effects are of concern in the ability of military vehicles and command post structures to withstand the effects of incident blast/thermal waves caused by nuclear bursts. The computational modeling of these effects utilize time-dependent Euler and Navier-Stokes techniques. A typical example of the problem of interest[17] is depicted schematically in Figure 20 where a vehicle is shown being struck by an incident blast wave. Reference 17 reported the application of an inviscid, finite-difference code to predict the time-dependent flow over several objects of generic interest. An example of the resulting sequence of density contours for the flow over the truck are shown in Figure 21. Fully three-dimensional viscous computations coupled with the effect of the thermal pulse are required to properly model the complex shapes and flowfield conditions of interest.

CLOSING REMARKS

A brief overview has been presented of the computational modeling applications and activities at the US Army Ballistic Research Laboratory. The topics covered are by no means complete. Several additional areas of active research are in progress. The scope of this paper was not intended to provide a complete coverage, only a partial coverage within the allowed constraints. Given the supercomputer resources now available at the BRL, the impact of computational modeling on weapon system design and development is certain to become significant.

REFERENCES

1. Pulliam, T.H. and Steger, J.L., "On Implicit Finite-Difference Simulations of Three-Dimensional Flow," AIAA Journal, Vol. 18, No. 2, February 1980, pp. 159-167.

2. Schiff, L.B. and Steger, J.L., "Numerical Simulation of Steady Supersonic Viscous Flow," AIAA Journal, Vol. 18, No. 12, December 1980, pp. 1421-1430.

3. Sturek, W.B. and Schiff, L.B., "Numerical Simulation of Steady Supersonic Flow over Spinning Bodies of Revolution," AIAA Journal, Vol. 20, No. 12, December 1982, pp. 1724-1731.

4. Nietubicz, C.J., Sturek, W.B. and Heavey, K.R., "Computations of Projectile Magnus Effect at Transonic Velocities," AIAA Journal, Vol. 23, No. 7, July 1985, pp. 998-1004.

5. Nietubicz, C.J., Inger, G.R. and Danberg, J.E., "A Theoretical and Experimental Investigation of a Transonic Projectile Flow Field," AIAA Paper No. 82-0101, January 1982.

6. Sahu, J., Nietubicz, C.J. and Steger, J.L., "Numerical Computation of Base Flow for a Projectile at Transonic Speeds," AIAA Paper No. 82-1358, August 1982.

7. Nietubicz, C.J., Pulliam, T.H. and Steger, J.L., "Numerical Solution of the Azimuthal-Invariant Thin-Layer Navier-Stokes Equations," AIAA Journal, Vol. 18, No. 12, December 1982, pp. 1411-1412.

8. Sahu, J., Nietubicz, C.J. and Steger, J.L., "Navier-Stokes Computations of Projectile Base Flow with and without Base Injection," AIAA Paper No. 83-0224, January 1983.

9. Weinacht, P., Guidos, B.J., Kayser, L.D. and Sturek, W.B., "PNS Computations for Spinning and Finned-Stabilized Projectiles at Supersonic Velocities," AIAA Paper No. 84-2118, August 1984.

10. Weinacht, P., Guidos, B.J., Sturek, W.B. and Hodes, B.A., "PNS Computations for Spinning Shell at Moderate Angles of Attack and for Long L/D Finned Projectiles," AIAA Paper No. 85-0273, January 1985

11. Gough, P.S., "Modeling of Rigidized Gun Propelling Charges," Contract Report ARBRL-CR-00518, US Army Ballistic Research Laboratory, Aberdeen Proving Ground, MD, November 1983.

12. Horst, A.W., Robbins, F.W. and Gough, P.S., "A Two-Dimensional, Two-Phase Flow Simulation of Ignition, Flamespread and Pressure-Wave Phenomena in the 155-mm Howitzer," ARBRL-TR-02414, US Army Ballistic Research Laboratory, Aberdeen Proving Ground, MD, July 1982.

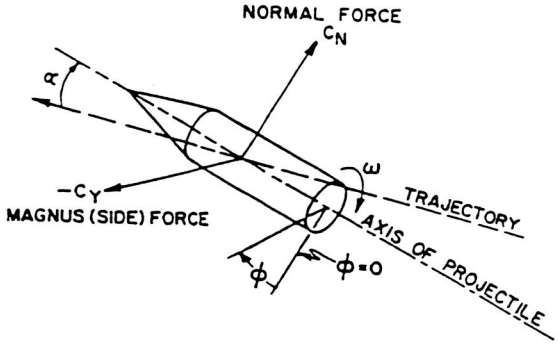

Figure 1. Aerodynamic Forces on a Spinning Shell

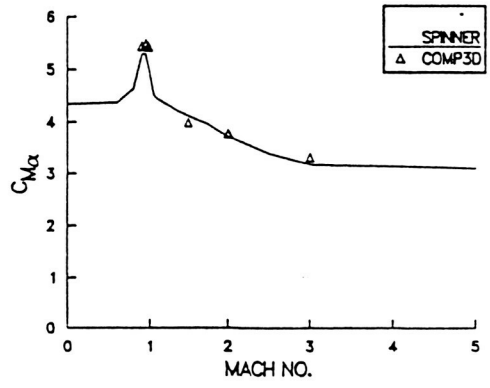

Figure 2. Critical Aerodynamic Behavior of a Boattailed Artillery Shell

13. Zukas, J.A., Jonas, G.H., Kimsey, K.D., Misey, J.J. and Sherrick, T.M., "Three-Dimensional Impact Simulations: Resources and Results," Computer Analysis of Large-Scale Structures, AND Vol. 49, edited by K.C. Park and R.F. Jones, Jr., published by ASME.

14. Johnson, G.R., BRL-CR-343, US Army Ballistic Research Laboratory, Aberdeen Proving Ground, MD, 1977.

15. Snow, P., "KEPIC-2," Kaman Sciences Corporation Report K82-46U (R), August 1982.

16. Kimsey, K.D. and Zukas, Jonas A., "Contact Surface Erosion for Hypervelocity Problems," ARBRL-MR-3495, US Army Ballistic Research Laboratory, Aberdeen Proving Ground, MD, February 1986.

17. Mark, A. and Kutler, P., "Computation of Shock Wave/Target Interaction," AIAA Paper No. 83-0039, January 1983.

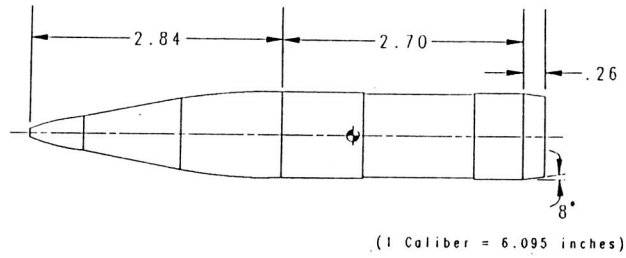

Figure 3. Simplified Geometry of the M483 Artillery Shell

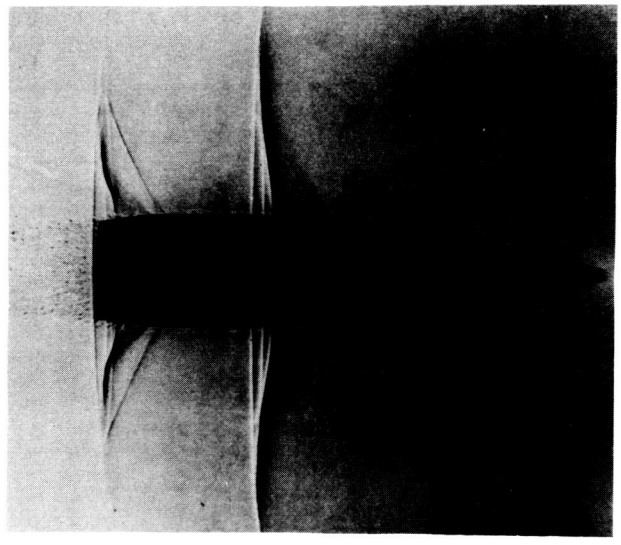

Figure 4. Spark Shadowgraph of a Shell in Flight at M = .96

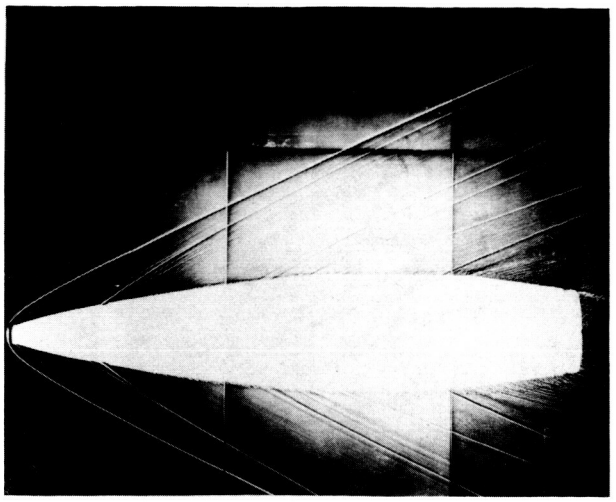

Figure 5. Spark Shadowgraph of a Shell in Flight at M = 2.3

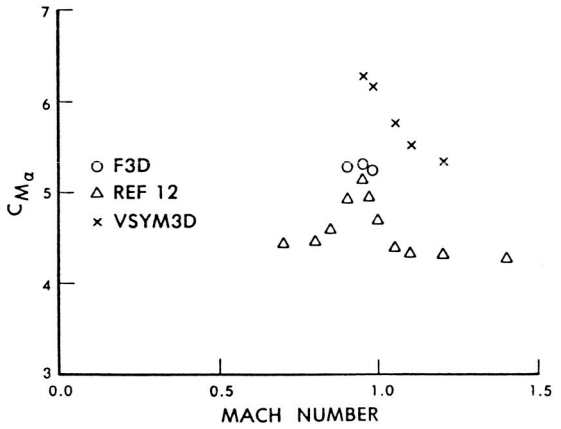

Figure 6. Pitching Moment Versus Mach Number for M549 Shell

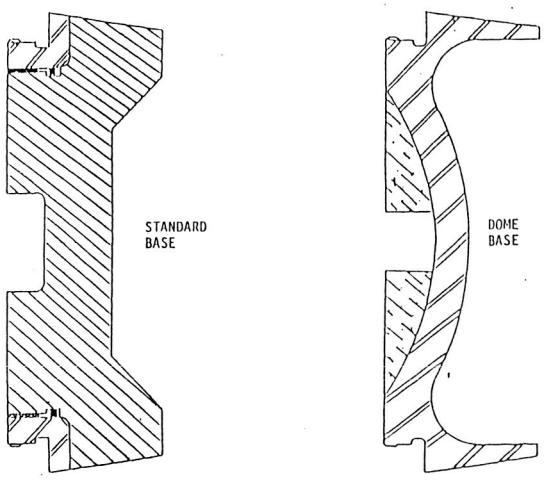

Figure 7. Standard and Domed Base Configurations for the M483

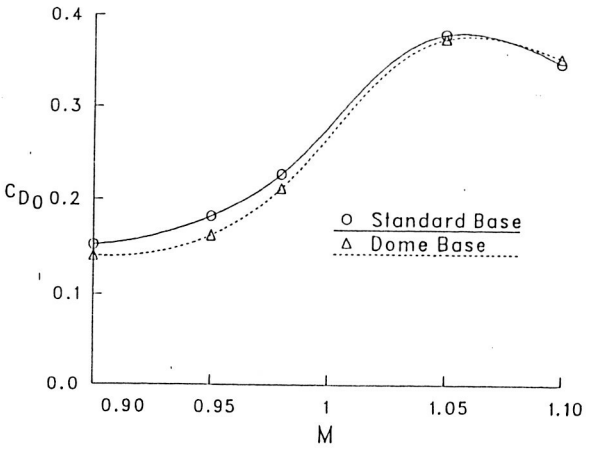

Figure 8. Total Drag Versus Mach Number for the Standard and Domed Bases, M483

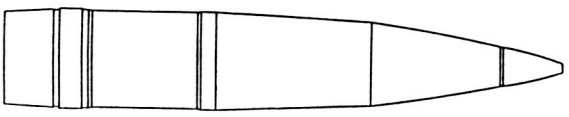

Figure 9. XM864 Base Bleed Shell

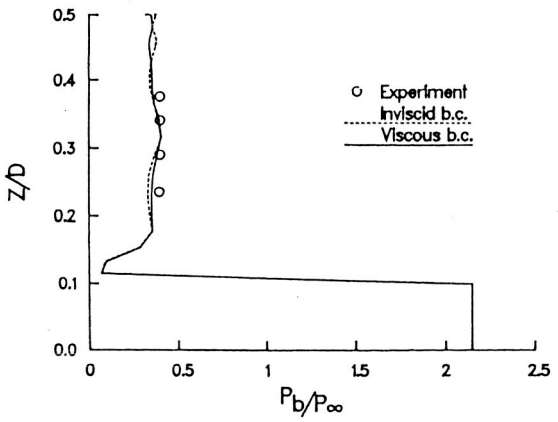

Figure 10. Base Pressure Predictions for the MICOM Test Case

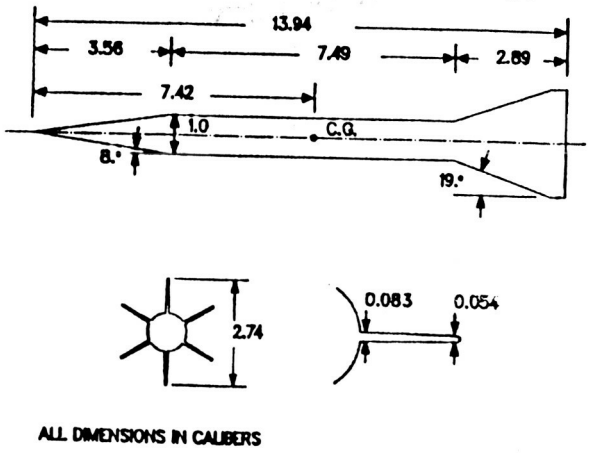

Figure 11. Simplified Geometry of the M735 KE Penetrator Projectile

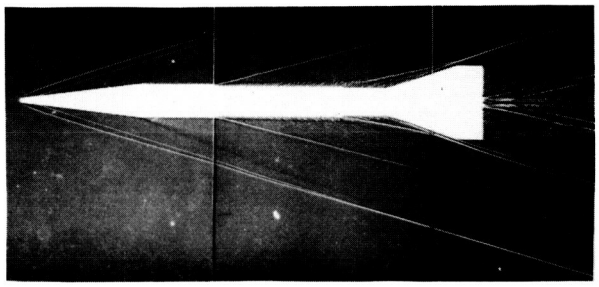

Figure 12. Spark Shadowgraph of Flight of M735 at Mach = 4.5

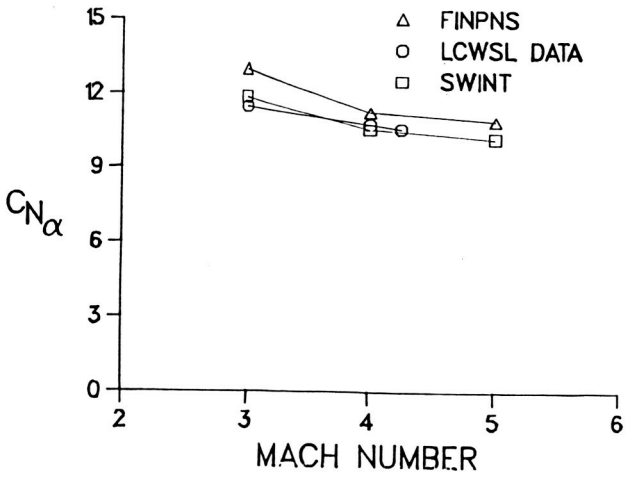

Figure 13. Slope of Normal Force Coefficient Versus Mach Number for M735

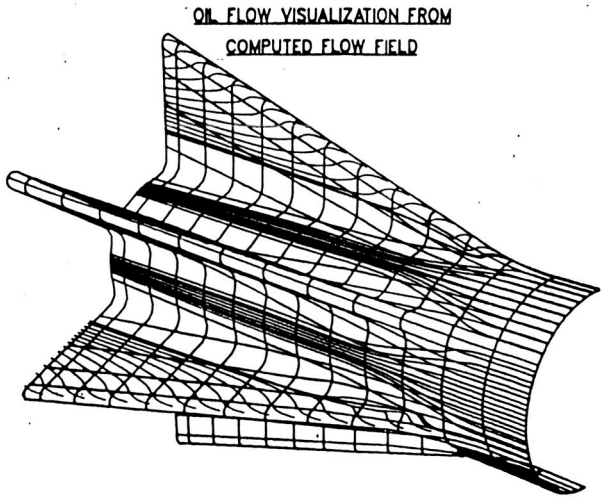

Figure 14. Surface Flow Patterns in Vicinity of Fins for M735 Geometry

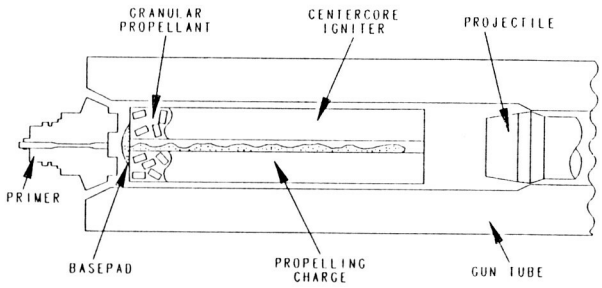

Figure 15. Schematic Illustration of a Bagged Charge/Gun Chamber Geometry

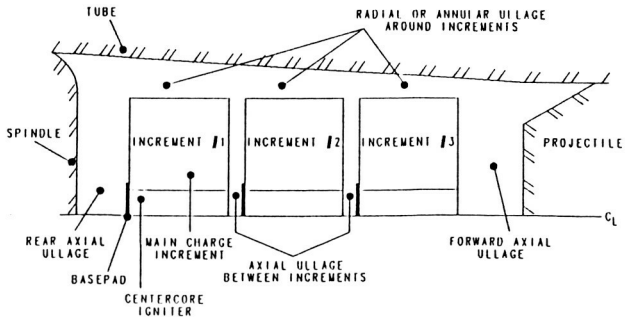

Figure 16. Schematic Illustration of a Multi-Increment Charge

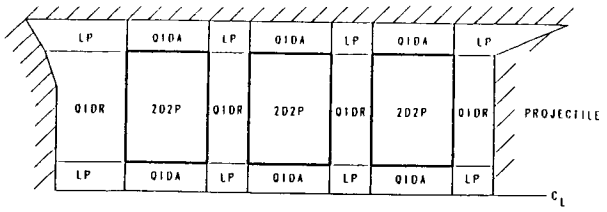

2D2P - TWO-DIMENSIONAL, TWO-PHASE
Q1DA - QUASI-ONE-DIMENSIONAL, AXIAL (SINGLE- or TWO-PHASE)
Q1DR - QUASI-ONE-DIMENSIONAL, RADIAL
LP - LUMPED PARAMETER

Figure 17. Modeling Techniques for Multi-Increment Charge

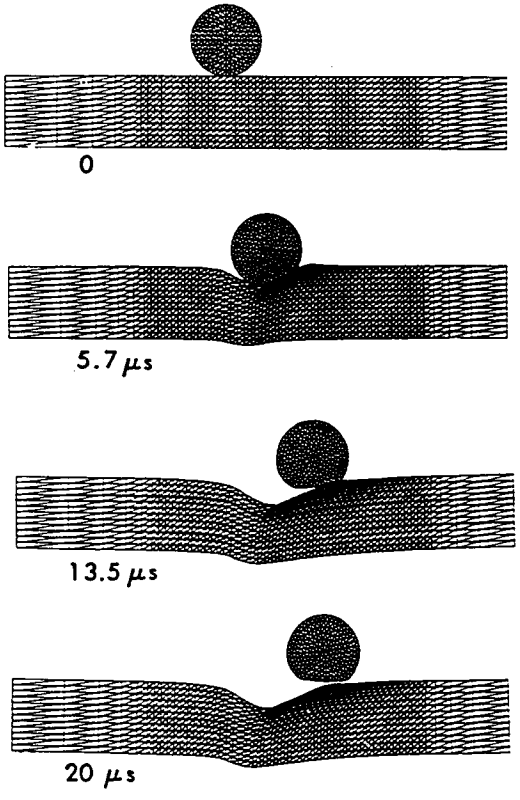

Figure 18. Impact of Steel Ball with Aluminum Plate

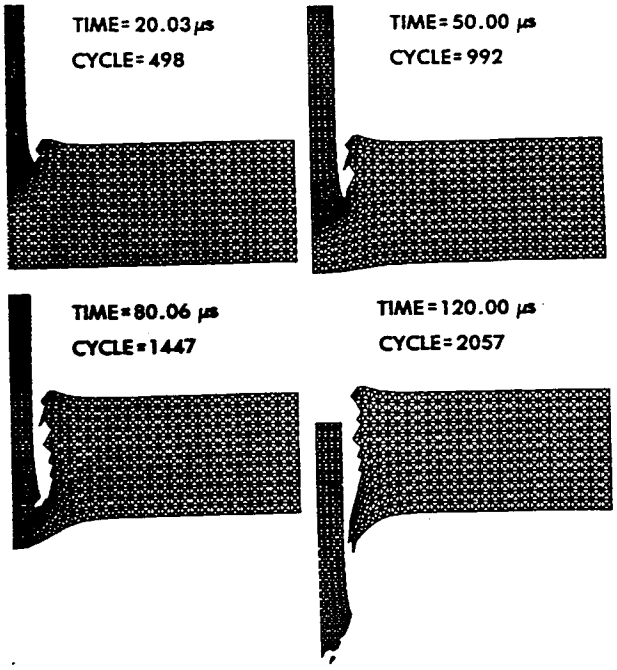

Figure 19a. Penetration of a Single Plate by a Long Rod

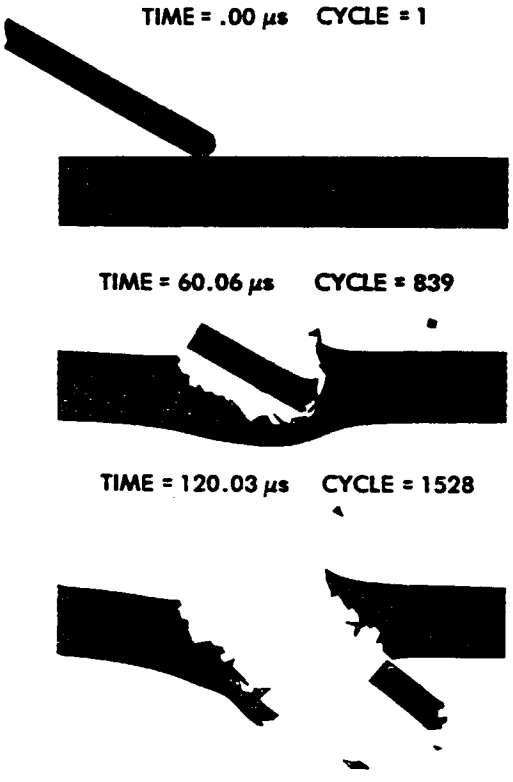

Figure 19b. Penetration of a Single Plate by a Long Rod

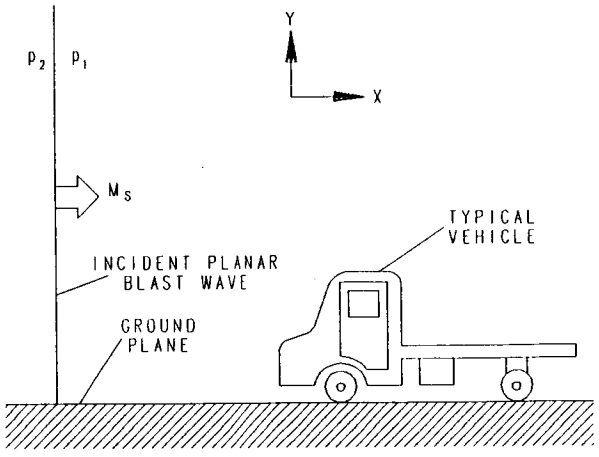

Figure 20. Schematic Illustration of a Vehicle-Blast Wave Interaction

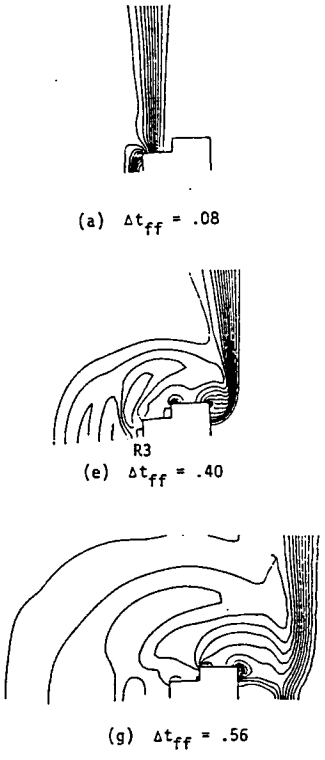

(a) $\Delta t_{ff} = .08$

(e) $\Delta t_{ff} = .40$

(g) $\Delta t_{ff} = .56$

Figure 21. Density Contours for Blast Wave-Vehicle Interaction